2024

A histological investigation of *Arceuthobium pusillum* infections in *Picea rubens* and *Picea glauca*

Sade K. McClean
Bowdoin College

A histological investigation of *Arceuthobium pusillum* infections in *Picea rubens* and *Picea glauca*

An Honors Paper for the Department of Biology

By Sade McClean

Bowdoin College, 2024

Table of contents

ABSTRACT 1

INTRODUCTION 1

Figure 1. Two examples of dwarf mistletoe aerial shoot of the species *Arceuthobium pusillum* on *Picea glauca* branches. 2

Figure 2. Diagram of the endophytic system of *Arceuthobium pusillum* within a host branch. 3

Figure 3. A single dwarf mistletoe seed (*A. pusillum*) moments before hydrostatically projected dispersal. 3

Figure 4. Example of a witch's broom caused by dwarf mistletoe (*A. pusillum*) on a Picea glauca tree. 4

Figure 5. North American Distribution of *Arceuthobium pusillum.* 5

METHODS 7

Site Selection 7

Figure 6. Collection site maps. 8

Sample Collection 8

Sectioning 8

Dual Staining 9

Light Microscopy and Data Collection 9

Figure 7. Illustrative and descriptive diagram of branch cross section from a *Picea rubens* tree that is infected with *Arceuthobium pusillum* (not a specific sample). 10

Figure 8. Imaging of *Picea* branches infected with *Arceuthobium pusillum* after dual staining with Safranin O and Aniline Blue. 10

RESULTS 10

Staining 11

Uninfected Samples 11

Occurrence Counts 11

Table 1. T-Test values from six different statistical tests comparing mean values from *Picea rubens* and *Picea glauca* branches infected with *Arceuthobium pusillum* 12

Figure 9. Mean number of *A. pusillum* infection occurrences in two tree species, *Picea glauca* and *Picea rubens* 12

Figure 10. Mean number of non-banded *A. pusillum* infections and banded *A. pusillum* infections of two tree species, *P. glauca* and *P. rubens* 13

Infection Area Relative to Branch Size 13

Figure 11. Mean of infected tissue area relative to originating cross section area from branches of *P. glauca* and *P. rubens* infected with *A. pusillum*, reported as percentages. 14

Area of Infection Interior relative to Cross Section Area 14

Figure 12. Mean percentages of the sum of each *A. pusillum* infection occurrences' interior area relative to its host branch's cross section area for two species of tree, *P. glauca* and P. *rubens* 15

Area of Banded Exterior Relative to Infection's Interior 15

Figure 13. Mean percentages of the area of each *A pusillum* infection occurrences' exterior band relative to the infection's contained interior for two species of tree, *P. glauca* and *P. rubens* 16

DISCUSSION **17**

ACKNOWLEDGEMENTS **19**

WORKS CITED **20**

Abstract

Arceuthobium pusillum is a hemiparasite that infects select *Picea* species. The hosts of *A. pusillum* do not experience the same symptoms of infection. *A. pusillum* infections are more fatal to *P. marinara,* and *P. glauca. P. rubens*, on the other hand, can survive longer with sustained infection. This presents itself as a contemporary issue because *P. glauca,* one of the parasite's most vulnerable hosts, was untethered from ecological competition when old growth forests were subjected to large scale anthropogenic disturbances. These disturbances allowed *P. glauca* to proliferate, with *A. pusillum* following. A deeper understanding of the host-species specific responses to *A. pusillum* infection can broaden general knowledge of parasitic growth and development while also potentially inspiring conservation techniques. This study took advantage of the intrinsic differences between host and parasite to visualize infections in *P. rubens* and *P. glauca*, highlighting differences in infection outcome. By illuminating lignin and callose within cross sections of infected *P. rubens* and *P. glauca* branches, it was revealed that *P. rubens* forms dense bands of cells around the cortical strands of infection. These bands form more frequently in *P. rubens* than in *P. glauca* and are of a significantly larger area in *P. rubens* than in *P. glauca* ($t(8)$, $p=0.003$, $p=0.005$). The discovery of the exterior bands is novel and exciting, as the bands are possibly made of callose and potentially facilitate *P. rubens* survival against *A. pusillum* infection. The foundational discoveries and results of this study should inspire, and warrant, further analysis.

Introduction

Dwarf mistletoes, members of the *Arceuthobium* genus, are widespread, hemiparasitic angiosperms. They are found across the world, following the distributions of their hosts in the *Pinaceae* and *Cupressaceae* families (Hawksworth and Wiens, 1996; Kuijt, 1955). Although a large group, dwarf mistletoes are distinguishable by certain characteristics. These include their ability to form complex endophytic systems and aerial shoots within and along host branch tissue (Figures 1 & 2). Infections originate from a single hydrostatically propelled seed that land on a young host branch (Figure 3) (Gray et al., 2022; Hawksworth and Wiens, 1996; Kuijt, 1955). Dwarf mistletoe infections disfigure the host tree. This disfigurement is known as a 'witch's broom', a conglomeration of dense and irregular, self-shading branches (Figure 4). Witches' brooms are a symptom of the parasite's ability to sequester host resources (Hawksworth and

Wiens, 1996; Kuijt, 1955; Tinnin et al., 1982). Although dwarf mistletoe infections are not systemic (i.e. they are confined to a host branch), branches that are infected and form witches' brooms impact the entire tree by consuming a disproportionate share of the tree's resources such as water, fixed carbon and nitrogen (Muir and Hennon, 2007; Reblin et al., 2006). Typically, after years of sustained and serious infection, the witches' brooms are all that remain before a tree succumbs fully (Hawksworth and Wiens, 1996; Muir and Hennon, 2007). While dwarf mistletoes often induce mortality in their hosts, the severity of infections, and their symptoms, vary greatly by host species and regional conditions (Eaton, 1931; Gray et al., 2022; Hawksworth and Wiens, 1996; Muche et al., 2022; von Schrenk, 1900).

Figure 1. Two examples of dwarf mistletoe aerial shoots of the species *Arceuthobium pusillum* on *Picea glauca* branches. Left image from Baker et al., 2016. Right image, Monhegan Island, Maine, 2023.

Eastern dwarf mistletoe, *Arceuthobium pusillum*, is a prolific species of dwarf mistletoe in North America. Eastern dwarf mistletoe is native to the northeastern United States and eastern Canada (Figure 5) (Baker et al., 2006; Hawksworth and Wiens, 1996; Kuijt, 1955). This species of dwarf mistletoe is a principal parasite of the spruce species *Picea mariana, P. glauca* and *P. rubens,* and its abundance largely follows the range and distribution patterns of these hosts (Figure 5) (Baker et al., 2006; Gray et al., 2022; Hawksworth and Wiens, 1996; Kuijt, 1955; Logan et al., 2013). Like other dwarf mistletoes, eastern dwarf mistletoe infection begins when a single hydrostatically projected seed successfully lands on the branch of an acceptable host (Figure 3) (Eaton, 1931; Gray et al., 2022; Hawksworth and Wiens, 1996; Thoday and Johnson, 1930). After the seed germinates it penetrates the host's cortex by creating a radicle (Dodds, 2022; F. G. Hawksworth and A. L. Shigo, 1980; Thoday and Johnson, 1930). After

successful penetration of the host cortex, the parasite is able to develop a complex endophytic system (Figure 2) (Dodds, 2022; Thoday and Johnson, 1930). The endophytic system of *A. pusillum* is made of a cortical strand growing along the cortex and phloem of the host tree, accompanied by sinkers that extend into the woody interior (xylem) of the host (Figure 2) (Thoday and Johnson, 1930). It is with this intricate, and root like, structure that eastern dwarf mistletoe can sequester resources from the host. With the endophytic system established, the mistletoe is set to grow and proliferate. Roughly four years after initial germination, the parasite is mature enough to grow aerial shoots, and is one step closer to repeating the cycle of infection (Dodds, 2022; Thoday and Johnson, 1930). Eastern dwarf mistletoe infects different host species with consistent, physiological mechanisms, though, like other dwarf mistletoes, the mortality rate of infection differs across host species (Baker et al., 2006; Muche et al., 2022; (Muche et al., 2022; Reblin et al., 2006).

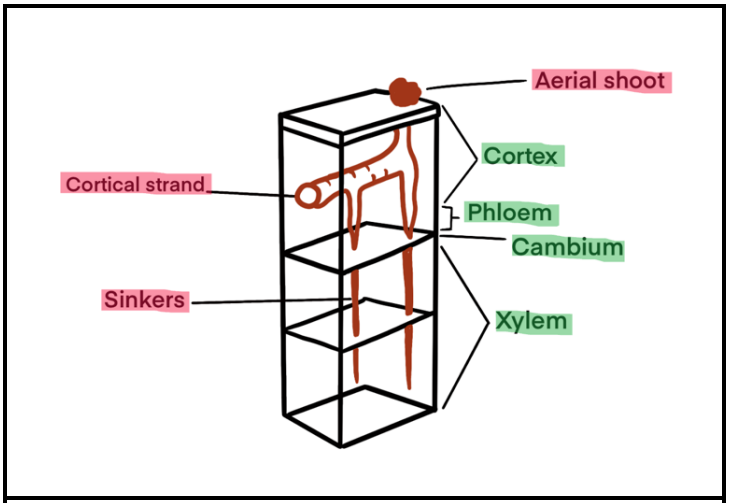

Figure 2. Diagram of the endophytic system of *Arceuthobium pusillum* within a host branch. Terms highlighted in red denote endophytic components. Terms highlighted in green denote structural components of the host branch.

Variability in infection intensity is thought to be largely due to host species responding differently to the parasite (Baker et al., 2006; F. G. Hawksworth and A. L. Shigo, 1980; Gray et al., 2022; Hawksworth and Wiens, 1996; Kuijt, 1955; Logan et al., 2013; Reblin et al., 2006; Stanton, 2006). For instance, eastern dwarf mistletoe infections are more fatal to black spruce trees,

Figure 3. A single dwarf mistletoe seed (*A. pusillum*) moments before hydrostatically projected dispersal. Pictured in the red circle. Monhegan Island, Maine, October 2023.

P. marinara, and white spruce trees, *P. glauca* (Baker et al., 2006; Gray et al., 2022; Logan et al., 2013). Infections have proven less fatal to red spruce trees, *P. rubens* (Baker et al., 2006; Hawksworth and Wiens, 1996; Logan et al., 2013; von Schrenk, 1900). Red spruce trees can survive longer with sustained infection than black spruce and white spruce trees (F. G. Hawksworth and A. L. Shigo, 1980). Red spruce trees are also known to shed infected branches, enabling them to survive past their initial infection (Baker et al., 2006; Hawksworth and Wiens, 1996). The physiological mechanisms that allow red spruce trees to withstand eastern dwarf mistletoe infection are unknown, though it is hypothesized that the parasite's impact on host water relations is mitigated in red spruce trees (F. G. Hawksworth and A. L. Shigo, 1980; Logan et al., 2013). For instance, it is possible that red spruce trees, being a more shade tolerant species than white spruce trees, have a lower baseline expenditure of carbon (Barton M. Blum, 1990; Reblin et al., 2006). This difference in uninfected, or baseline, resource usage may mean that red spruce trees have a greater capacity to tolerate the parasite actively sequestering its resources than white spruce trees do, allowing them to withstand the infection (Logan et al., 2013).

Figure 4. Example of a witch's broom caused by dwarf mistletoe (*A. pusillum*) on a Picea glauca tree. Picture, red circle. Monhegan Island, Maine, October 2023.

Eastern dwarf mistletoe infections in red spruce and white spruce trees are not a modern phenomenon, there is a long historical record of eastern dwarf mistletoe's influence across the northeast and specifically, within coastal Maine, though it has only recently become an issue for forests' integrity (Eaton, 1931; Jack, 1900; Norton, 1907; von Schrenk, 1900). Eastern dwarf mistletoe was first documented on black spruce trees (*P. marinara*) around 1870 in New York State. After its initial discovery and description, there was a period of disinterest in the mistletoe as it was not a prolific parasite at the time (Jack, 1900; von Schrenk, 1900). That was, until infections were found in unprecedented places and abundances around New England in the 20th

century. Eastern dwarf mistletoe transitioned from a native, seemingly unnoticeable parasitic plant in the nineteenth century, to being wildly destructive by the mid twentieth century. This was largely because white spruce, one of eastern dwarf mistletoes most vulnerable hosts, was untethered from ecological competition when old growth forests were subjected to large scale agricultural disturbances (Eaton, 1931; Norton, 1907; von Schrenk, 1900). This allowed white spruce to proliferate, expanding eastern dwarf mistletoes host range and thereby enabling the parasites own proliferation. Because eastern dwarf mistletoe, was, historically, not a particularly destructive plant, specific interactions between this parasite and its primary hosts were not well studied, but there is a growing need for research as eastern dwarf mistletoe continues to ravage forests at a historically unprecedented level (de Lafontaine et al., 2010; Hawksworth and Wiens, 1996; Kuijt, 1955; Logan et al., 2013; Nowacki et al., 2010; Reblin et al., 2006).

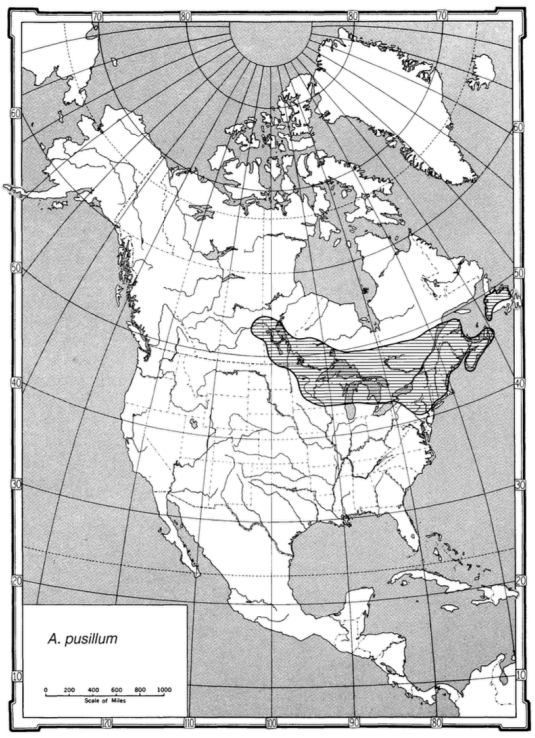

Figure 5. North American Distribution of *Arceuthobium pusillum.* From Hawksworth and Wiens 1996.

Homogenous forest stands of white spruce are more vulnerable to devastation than more diverse stands, as in the monoculture effect (Felton et al., 2016). Homogenous white spruce stands, while rare across the rest of the United States, are common on Maine's headlands and islands specifically because of the unique climate and its history of centuries of agricultural use and timber harvesting that abruptly ended in the early the twentieth century (Cogbill, 2013). White spruce, being shade intolerant, was historically unable to establish itself in great abundance due to the existence of heavily shaded old growth forests prior to colonial settlement (Hans Nienstaedt and John C. Zasada, 1990; Reblin et al., 2006; Tolonen, 1983). After pre-colonial forests were cleared for agricultural purposes and subsequently deserted, the same land that was once heavily shaded by old trees was suddenly saturated with sunlight. This enabled the establishment of homogenous white spruce trees in coastal Maine (de Lafontaine et al., 2010;

Hans Nienstaedt and John C. Zasada, 1990). The shift in forest composition, from heterogenous old growth forests to early successional and largely homogenous stands of white spruce, has left forests in coastal Maine and the rest of New England vulnerable to disturbances, particularly those that are species specific (Felton et al., 2016). This is especially true of the parasitic eastern dwarf mistletoe which, today, can ravage forests in an unprecedented manner given the higher abundance of its most sensitive principal host (Davis, 1966; Felton et al., 2016).

Given the evolution of eastern dwarf mistletoe's ecological impact and its current status as a destructive parasite, a more extensive exploration of the anatomy of infected host trees is called for (Mudgal et al., 2022). It would be particularly impactful to analyze red spruce trees and their response to eastern dwarf mistletoe, as it compares to the response of white spruce trees. This would strengthen the general understanding of host-parasite relationships as it relates to host-species differences. It could also inform conservation efforts of white spruce stands and, potentially, preventative conservation of other vulnerable species (Mudgal et al., 2022).

As an angiosperm, eastern dwarf mistletoe has fundamentally different anatomy than red spruce and white spruce trees, as they are gymnosperms. For instance, the relative amount of lignin, a structural polymer found in plants, differ greatly between angiosperms and gymnosperms. Gymnosperms have a higher relative lignin content than angiosperms (Spaulding, 1906; Spaulding, 1906; Zhang et al., 2022). As such, it is possible to utilize histochemical staining to highlight differences in features such as lignin, to differentiate host and parasite (Brown, 1961; Currier, 1957; Evert and Derr, 1964; Kutscha and Gray, 1972; Li et al., 2023; Nikolov et al., 2014; Spaulding, 1906). Additionally, under the conditions of infection, the host trees are gymnosperms under biotic stress. When plants experience stress, including of a parasitic nature, they are known to respond with callose depositions (Chen and Kim, 2009; Currier, 1957; Li et al., 2023; Poovaiah, 1974; Wang et al., 2021). Callose depositions can function to 'seal off' and contain pathogens or parasites from infiltrating other areas of the host. By utilizing histological staining to analyze callose content, it is possible to assess the differences between the infection responses of red spruce and white spruce trees. With histochemical staining, qualities of eastern dwarf mistletoe infection and response of the host tree can be measured and quantified with imaging (Brown, 1961; Cochrane and Ford, 1978; Currier, 1957; Kutscha and Gray, 1972; Muche et al., 2022; Nikolov et al., 2014; Srebotnik and Messner, 1994). Staining for lignin enables the visualization of uninfected host tissue, while staining for callose content

enables the visualization of the hosts' response to the infection. Analysis of the differences between stained, infected branch cross sections, can provide valuable information about the physical defenses host species implement in the face of *A. pusillum* infection and what leads white spruce trees to succumb to infection while red spruce trees manage to withstand it.

Methods

Site Selection

Monhegan Island, Maine, was used as the initial site for the collection of *A. pusillum* infected red spruce and white spruce branch samples because of its uniquely well documented history of land use and land management (Figure 6). Its rich historical record allows this analysis of parasite-host relationships to also reflect post agricultural reforestation's impact on parasites' proliferation (Foster et al., 2002). One of the earliest firsthand reports of vegetation on Monhegan Island dates to the year 1605 and the landing of George Waymouth (Tolonen, 1983). During his travels, Waymouth wrote that Monhegan was "woody, grouen with Firre, Birch, Oke and Beech, as farre as we saw along the shore; and so likely to be within" (Rosier, James and Burrage, Henry, S., 1887, 95). Waymouth's account of Monhegan Island's vegetation is incongruent with what is found today. All that is left of the virgin, old growth tree stands, like that which were viewed by Waymouth on Monhegan in 1605, are known as the "Cathedral Woods" (Figure 6).

The contrast of Waymouth's record to modern reports reflects this broad change in the composition of coastal Maine's forests from rich and biologically diverse habitats to more homogenous stands of opportunistic species (Cogbill, 2013; Davis, 1966; Lorimer, 1977). The impacts of anthropogenic disturbances are exaggerated on Monhegan Island with the juxtaposition of the younger, white spruce forests, with the untouched "Cathedral Woods" that is still largely populated by shade tolerant and later successional species such as red spruce (Figure 6**)** (Barton M. Blum, 1990; Reblin et al., 2006). The proximity of old growth forests that contain red spruce trees to newer, early successional forests that are mainly white spruce stands, on Monhegan Island, lends it to be an exceptional site to compare how eastern dwarf mistletoe infections manifest in red spruce and white spruce trees.

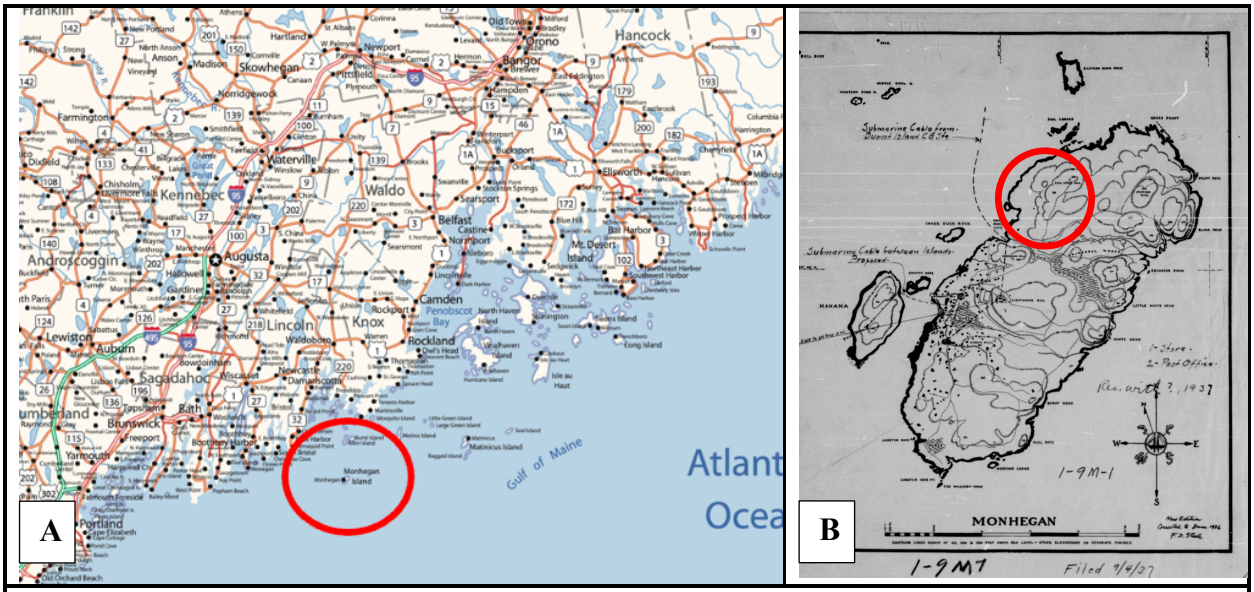

Figure 6. Collection site maps. Left (A) shows the site of sample collection, Monhegan Island, Maine (red circle), relative to the coast of Maine from Brunswick to Columbia Falls. From etravelMaine.com. Right (B) is a map of Monhegan Island and its Cathedral Woods, outlined with the red circle. From the Cartographic and Architectural National Archives, 1937.

Sample Collection

Ten branch clippings of ~12 inches were removed from different red spruce and white spruce trees (20 total). Five infected and five uninfected branches were collected from each species of spruce. These samples were collected from Monhegan Island, Maine in October 2023 (Figure 6). Additional branch samples from uninfected red spruce trees were collected from the 'Bowdoin Pines' in Brunswick, Maine in February 2024. Branch trimmings were removed using gardening shears and refrigerated at 4° C until they were sectioned.

Sectioning

To standardize cross sections by age, whorls of each branch sample were counted, starting from the terminal bud, to estimate segments of branch growth from three years ago (Cochrane and Ford, 1978). The segments of branches were trimmed down into 3cm long pieces and measured for diameter. Pieces did not require embedding prior to sectioning. The woody tissue of the branches and the short time between initial sampling and sectioning led to cross sections maintaining structural integrity and quality (Lux et al., 2005). A Microm HM35S rotary microtome was used to cut each 3cm piece into 120 µm thick cross sections. While sectioning

was continuous, every 10th section was kept for further analysis, for a total of 25 sections per branch type (250 total sections).

Dual Staining

All the branch cross sections were double stained with Safranin O and Aniline Blue. Under light microscopy, Safranin O stains and defines lignified cells with red while Aniline Blue stains and defines un-lignified cells and other molecules, such as callose, with blue (Cochrane and Ford, 1978; Kutscha and Gray, 1972; Mulyaningsih et al., 2022; Nikolov et al., 2014; Thomas et al., 1894). Trial runs of staining techniques narrowed down methods to the following. During the initial staining of Safranin O, sections were submerged in a 0.2% Safranin O solution and rinsed with ethanol, according to the technique in Mulyaningsih et al., 2022. For the secondary staining, sections were submerged in a 0.05% solution of Aniline Blue for a longer period of up to 20 hours and then rinsed repeatedly with ethanol, according to the methods in Conti et al., 1983.

Light Microscopy and Data Collection

Of the 25 stained sections from each branch treatment ten complete sections were selected and mounted for analysis under a standard compound microscope (Olympus CHBS). Sections were mounted in water and images of each slide were taken using a phone mount. A series of photos were taken to capture the entirety of each mounted section. Photos were later analyzed using ImageJ to quantify the area of the infections' interiors and the infections' exterior bands within each section (Figures 7 & 8). For statistical analysis, each sample branch reflected the average values of its ten selected cross sections. T-tests were used to statistically compare the mean values for red spruce and white spruce branches.

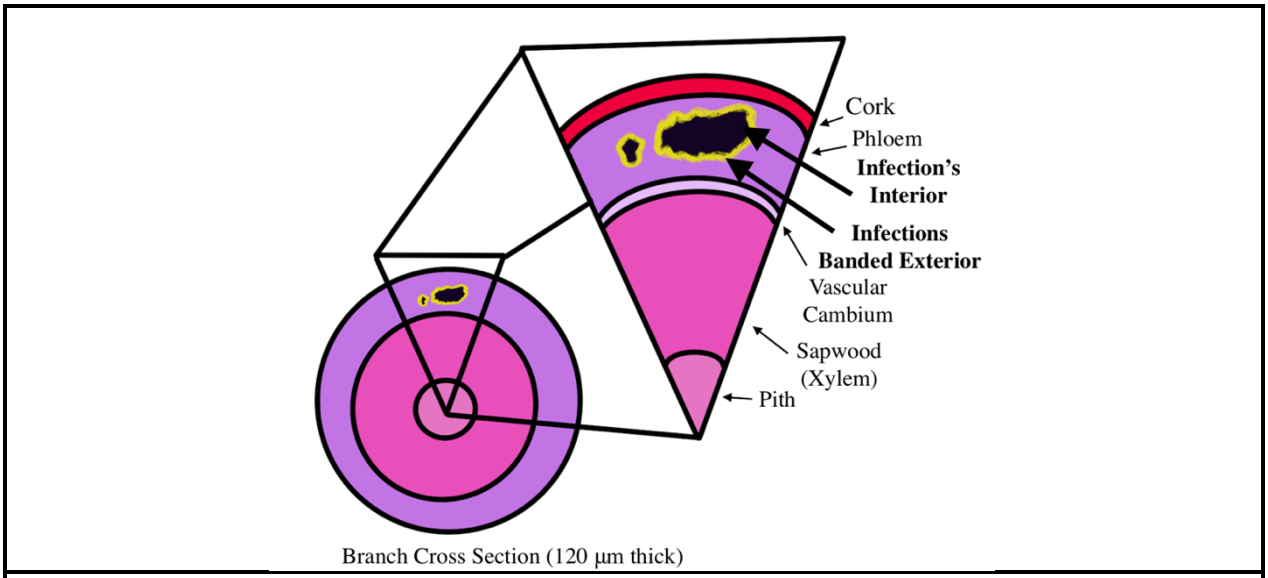

Figure 7. Illustrative and descriptive diagram of branch cross section from a *Picea rubens* tree that is infected with *Arceuthobium pusillum* (not a specific sample). Non bolded labels identify major, known, components of *P. ruben's* structural composition. Bolded labels identify components of *A. pusillum* infection defined in this study. Infection's banded exterior is defined as the lighter and distinct strip of cells encompasing the darkened cells of the infection interior. Colors of the section diagram resemble the results of *Picea* branch cross section dual staining with Safrinin O stains and Aniline Blue.

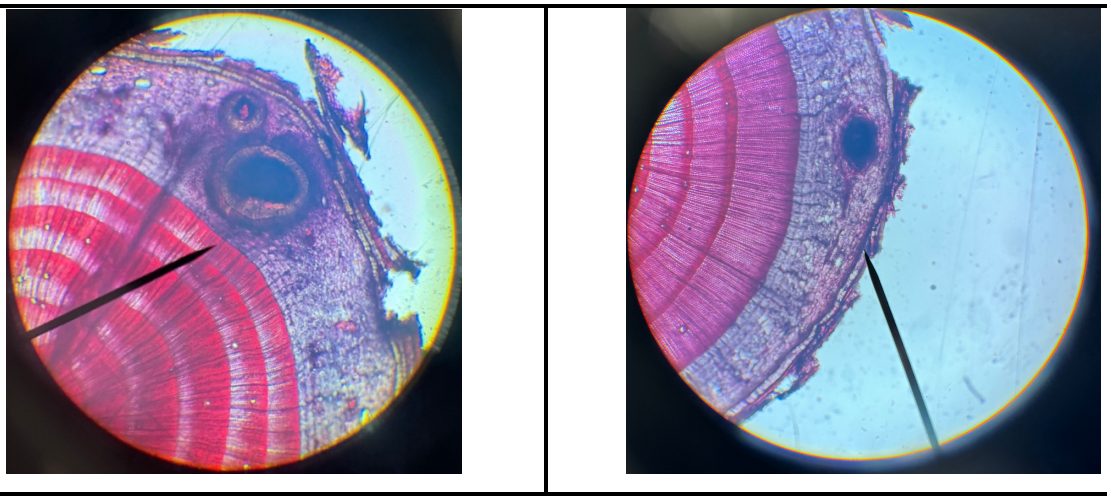

Figure 8. Imaging of *Picea* branches infected with *Arceuthobium pusillum* after dual staining with Safranin O and Aniline Blue. Left, image of *Picea rubens* branch 4, section number 1. Two clear examples of infection occurrences are pictured in this sample. The infection occurrences exterior bands are stained yellow/green while the infections interior is the darkened center of the band. Phloem is stained blue/purple while xylem is stained red. Right, image of *Picea glauca* branch 5, section number 6. One clear example of an *Arceuthobium pusillum* infection occurrence lacking a banded exterior. The infection is the darkened amalgamation of cells. Phloem is stained blue/purple while xylem is stained red.

Results

Staining

The staining of cross sections was successful (Figure 8). It was concluded through cross analysis with known structural and compositional features of woody tissue, that the colors retained in this study's samples, were congruent with the appropriate stains' use (Figure 7 & 8).

Uninfected Samples

Stained cross sections from uninfected red spruce and white spruce trees were imaged and analyzed. Data from the uninfected branches were used as a control to confirm the anomalies in the cross sections that were caused by the eastern dwarf mistletoe (Figures 7 & 8). Data from uninfected branches are not reflected in the results, which focus upon host specific differences in infection.

Occurrence Counts

Mean number of cortical strands in branches of infected red spruce and white spruce trees were calculated (Figures 2 & 9). One infection occurrence was defined one cortical strand with or without a banded exterior (Figures 7 & 8). The difference in mean number of infection occurrences or cortical strands for red spruce and white spruce was not statistically significant, but red spruce branches did, on average, had slightly more infections (3.8 vs 3.6) (Figure 9, Table 1). The mean number of banded and un-banded cortical strands were also calculated for each tree species (Figure 10). *P. glauca* branches, on average, had fewer infection occurrences that were banded, 0.29 vs 3.03, respectively. *P. rubens* branches on the other hand, had a greater number of infection occurrences with bands than without, 2.88 vs 0.82, respectively. Red spruce trees had more banded infections than white spruce trees, though this trend just exceeded the threshold for statistical significance ($t(8)$, $p=0.053$) (Figure 10, Table 1). White spruce branches had a significantly larger number of non-banded infection occurrences than red spruce branches ($t(8)$, $p=0.005$) (Figure 10, Table 1).

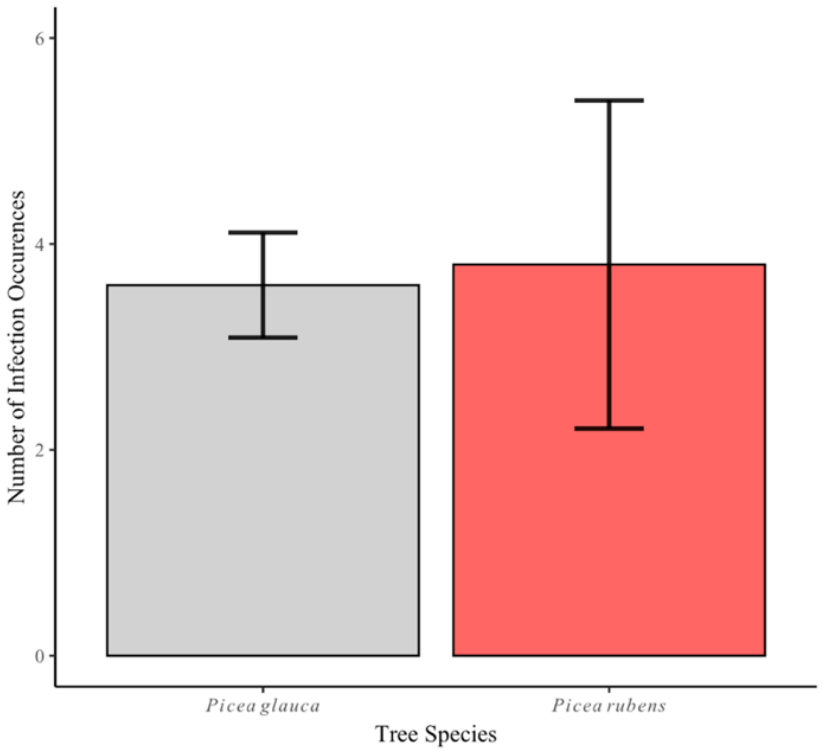

Figure 9. Mean number of *A. pusillum* infection occurrences in two tree species, *Picea glauca* and *Picea rubens*. No significant difference between the two means (t(8) p = 0.908). Gray and red bars represent the mean count of infection occurrences from *P. glauca* and *P. rubens* respectively. Black lines represent mean ± se. Mean ± se of the number of infection occurrences for *P. glauca* and *P. rubens* were 3.6 ± 0.5 and 3.8 ± 1.6 respectively. A single infection occurrence was counted for each cluster of deeply stained and concentrated cells in the phloem, presence of band was not considered. Mean count for both tree species were calculated from the mean count of infection occurrences of five independent branch samples' (n=5). The five branch samples' mean count of infection occurrences were calculated from infection occurrence counts of 10 different cross sections (n=10).

	mean				
	Picea rubens	*Picea glauca*	*df*	*t*	*p*
Number of Infections	3.800	3.6000	8	0.12	0.908
Infection Area/Branch Area	0.008	0.0020	8	2.52	0.036
Area of Infections' Interior/Branch Area	0.005	0.0018	8	1.83	0.105
Band Area/Infections' Interior Area	0.710	0.1300	8	4.25	0.003
Number of Banded Infections	2.880	0.2930	8	2.27	0.053
Number of Non-Banded Infections	0.820	3.0300	8	-3.78	0.005

Table 1. T-Test values from six different statistical tests comparing mean values from *Picea rubens* and *Picea glauca* branches infected with *Arceuthobium pusillum*. Red p values indicate statistically significant values, black are insignificant. Mean values were calculated from five independent branches' means. Branch means were calculated from 10 cross sections' data points. Each statistical test is reflected in graphical figures 9-13.

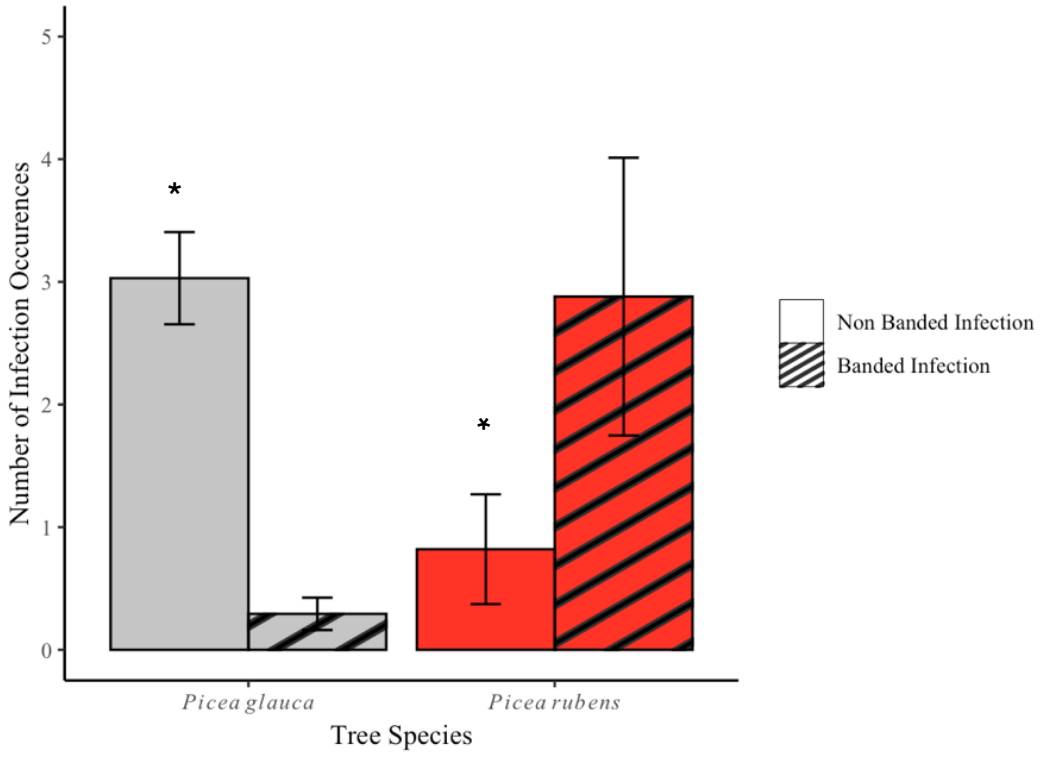

Figure 10. Mean number of non-banded *A. pusillum* infections and banded *A. pusillum* infections of two tree species, *P. glauca* and *P. rubens*. Gray and red clustered bars represent the mean count of infection occurrences for *P. glauca* and *P. rubens* respectively. Pattern denotes band status of the counted occurrences. Infections with a banded exterior are portrayed with stripes and infections without a banded exterior are portrayed with solid color. Black lines represent mean ± se. Mean ± se counts of infection for un-banded and banded occurrences for *P. glauca* were 3.03 ± 0.37 and 0.29 ± 0.13 respectively. Mean ± se counts of infection for un-banded and banded occurrences for *P. rubens* were 0.82 ± 0.45 and 2.88 ± 1.13. Red spruce trees had more banded infections, though insignificantly (t(8), p= 0.053) (table 1). White spruce trees had a significantly larger amount of non-banded infections, denoted with star (t(8), p=0.005) (table 1).

Infection Area Relative to Branch Size

The average area of infected cross section, relative to shoot cross-sectional area for both *Picea glauca* and *Picea rubens* cross sections were calculated as a percentage (Figure 11). Infection area measured was inclusive of the banded exterior if present (Figure 6). *Arceuthobium pusillum* infection, on average, consumed a larger portion of white spruce cross sections than red spruce cross sections (t(8) 0.036) (Figure 11) (Table 1).

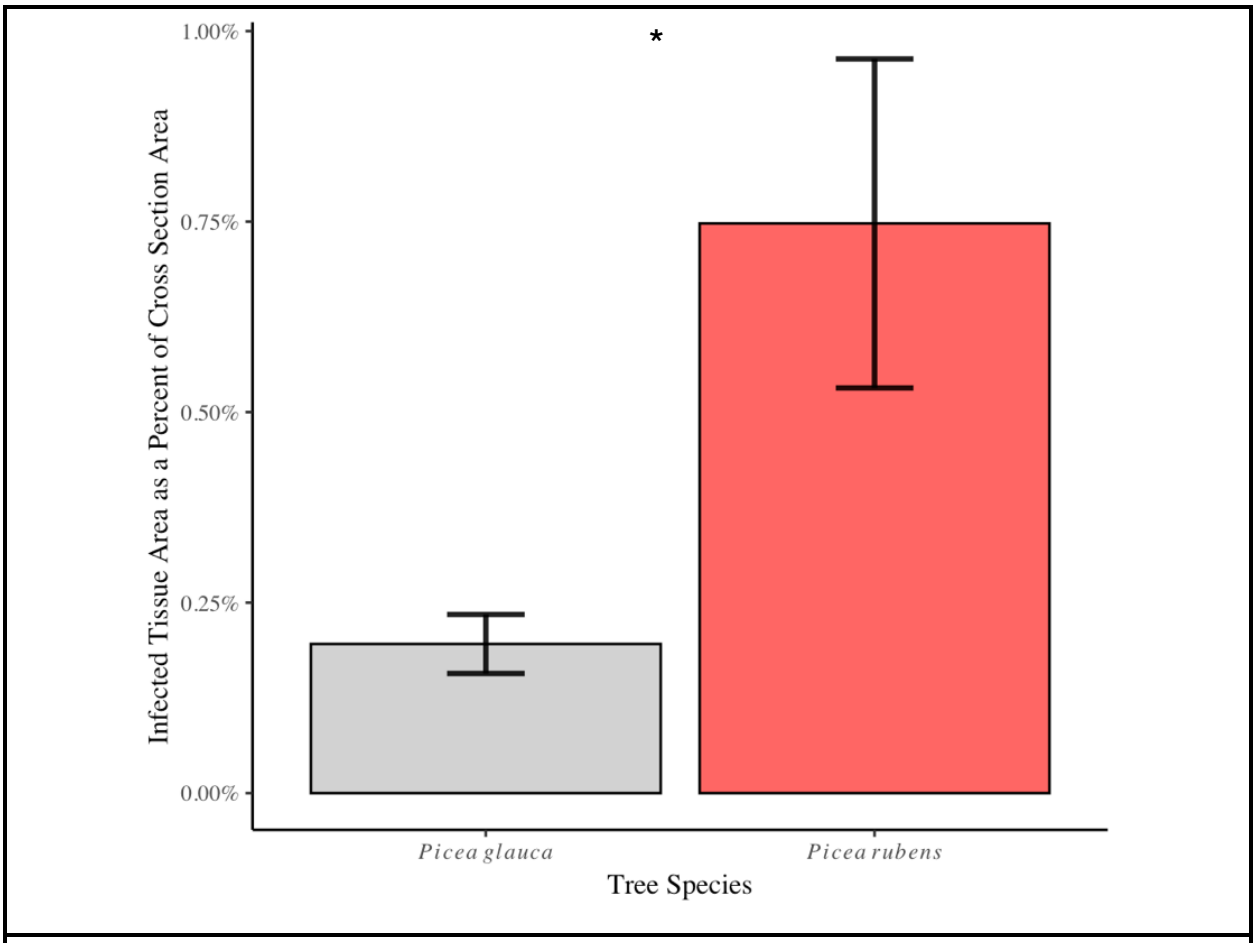

Figure 11. Mean of infected tissue area relative to originating cross section area from branches of *P. glauca* and *P. rubens* infected with *A. pusillum*, reported as percentages. Tissue from cross sections of *P. rubens* that was infected occupied significantly larger area than that of *P. glauca*, denoted with star (t(8) p=0.036). Gray and red bars represent the mean of the summed area (mm^2) of each infection occurrence, within a cross section, as a percent of the whole cross section's area (mm^2) from branches of *P. glauca* and *P. rubens*. Black lines represent mean percentage ± se. Mean ± se of the summed area (mm^2) of each infection occurrence as a percent of the cross sectional area (mm^2) were 0.75% ± 0.22% and 0.19% ± 0.04%. The means by tree species were calculated from the means of five branches of each species (n=5). Each branch's mean was calculated from the summed area (mm^2) of each infection occurrence as a percent of the whole cross section's area (mm^2) of 10 different cross sections for each branch (n=10).

Area of Infection Interior relative to Cross Section Area

The average area of each infection's interior, relative to its cross-section area for both *Picea glauca* and *Picea rubens* were calculated as a percentage (Figure 12). Infection area did not include the banded exterior if present. There was no significant difference in the mean area of

the infections' interiors relative to the cross sections' areas between *Picea rubens* and *Picea glauca* (Figure 12) (Table 1).

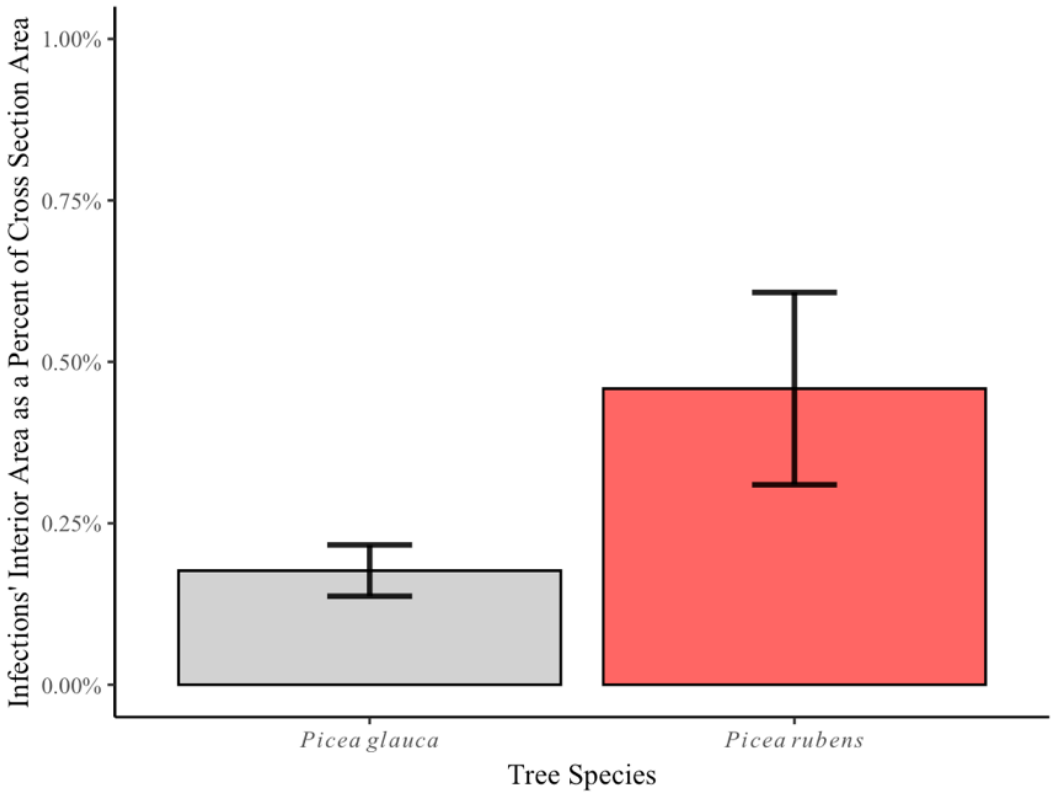

Figure 12. Mean percentages of the sum of each *A. pusillum* infection occurrences' interior area relative to its host branch's cross section area for two species of tree, *P. glauca* and P. *rubens.* No significant difference (Table 1). Gray and red bars represent the mean of the summed area (mm^2) of the infection interiors as a percent of the host branch's cross section area (mm^2) for *P. glauca* and *P. rubens* branches infected with Eastern Dwarf Mistle toe. Black lines represent mean ± se. The mean ± se of the summed area (mm^2) of infection interiors as a percent of the host branch's cross section area for *P. glauca* and *P. rubens* were 0.18% ± 0.04% and 0.45% ± 0.15% respectively. The means of the sum of the infections' interior areas (mm^2) as a percent of the host branches' cross section areas for each tree species were calculated from the means of five branches for each tree species (n=5). Each branch's mean value was calculated from the sum of the infections interior areas (mm^2)/the cross sectional area (mm^2) of 10 different cross sections of the branch (n=10).

Area of Banded Exterior Relative to Infection's Interior

The mean area of the infections' banded exterior relative to the infections' banded interior were calculated as percentages for branches of *P. glauca* and *P. rubens* infected with *A. pusillum* (Figure 13). On average, the banded exterior portions of infections, were of a greater area in red spruce cross sections than in white spruce cross sections (t(8), p=0.003) (Figure 13) (Table 1).

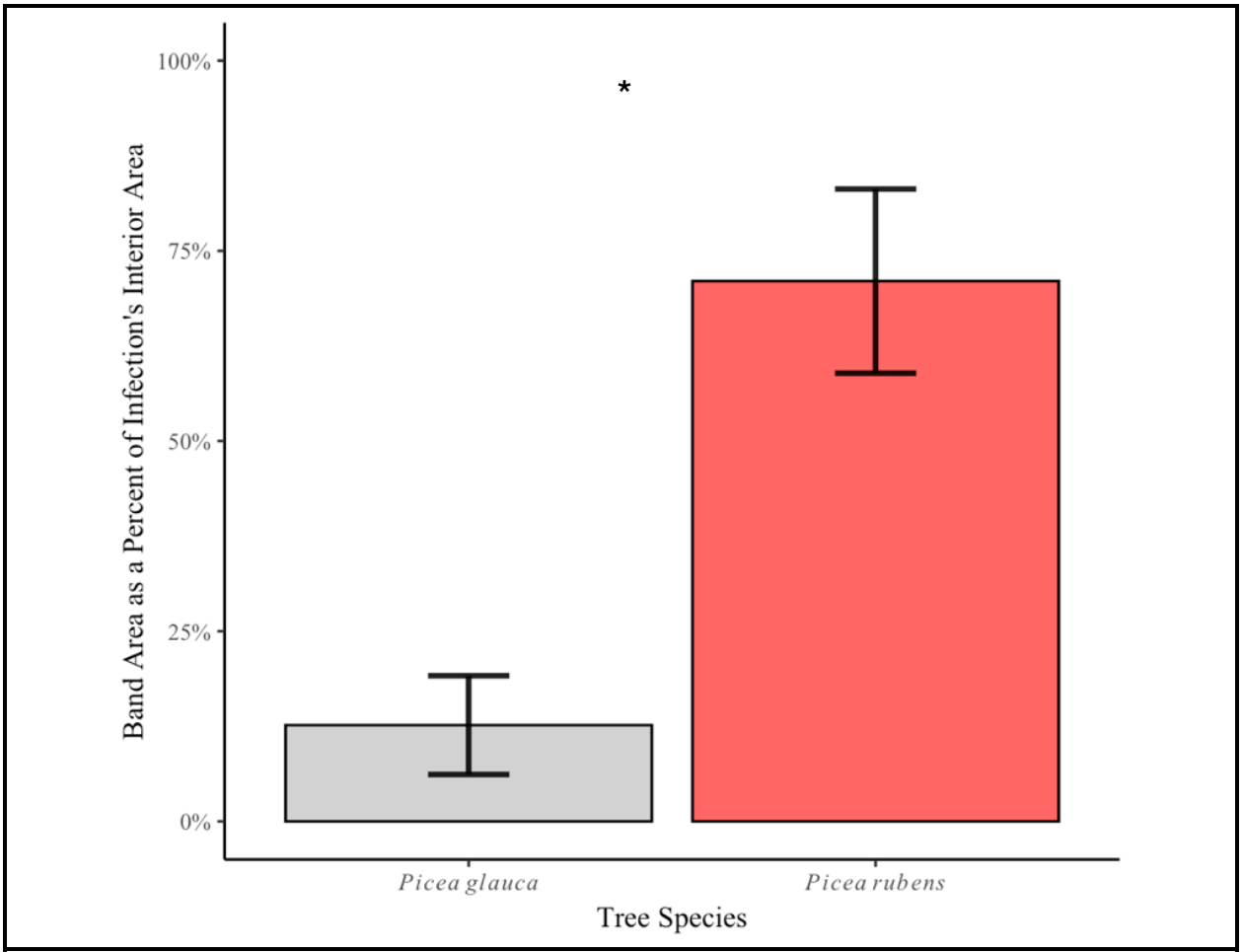

Figure 13. Mean percentages of the area of each *A pusillum* infection occurrences' exterior band relative to the infection's contained interior for two species of tree, *P. glauca* and *P. rubens.* Infection exteriors were significantly larger relative to infection interiors in *P. rubens* than *P. glauca,* denoted with star (t(8), p=0.003) (Table 1). Gray and red bars represent the mean of the area (mm^2) of each infection occurrences exterior band as a percent of the infection occurrence's interior area (mm^2) for *P. glauca* and *P. rubens* branches infected with *Arceuthobium pusillum*. Black lines represent mean ± se. The Mean ± se of the area (mm^2) of each infection occurrences exterior band as a percent of the infection occurrence's interior area (mm^2) for *P. glauca* and *P. rubens* were 12.65 ± 6.48% and 71.02 ± 12.12% respectively. The means of the area of each infections' exterior band area (mm^2) as a percent of the infections interior area for each tree species were calculated from the means of five branches for each tree species (n=5). Each branch's mean value was calculated from the sum of the infections interior areas (mm^2)/the cross sectional area (mm^2) of 10 different cross sections of the branch (n=10).

Discussion

This study identified host-species specific differences in the appearance of *Arceuthobium pusillum* infection by utilizing histological staining. Our study identified infection occurrences within branch cross sections using methods described in Lye (2006). This included the identification of parasite cell clusters by density and location within the cross sections. It was observed that *P. rubens* forms large groupings of cells around the localized site of the infections' cortical strands. Data from our study shows that *P. rubens* forms these bands more frequently than *P. glauca* branches do. Additionally, the bands are significantly thicker relative to the contained infection's center in *P. rubens* branches than in *P. glauca*. The bands themselves were consistently a yellow/green color, indicating that they are possibly formed of callose. This unique color could be caused by Safranin O staining callose a yellow hue and Aniline blue staining the callose and un-lignified cells, blue as well. Resulting in a dark yellow/green color (Mulyaningsih et al., 2022; Poovaiah, 1974). If the bands indicate callose depositions around the infection, that would have implications in terms of the wounding responses each host tree species implements. The possible callose rings could serve to slow the rate of parasitic growth as literature suggests (Li et al., 2023; Poovaiah, 1974; Wang et al., 2021). If this is the case, and the host tree is encompassing the invading parasite's cortical strand tissue with callose, that could help explain the discrepancy in mortality rates between *rubens* and *P. glauca* infected with *A. pusillum.* If the yellow bands around sites of infection are callose, *P. rubens* is potentially 'containing' the *A. pusillum* infection, slowing its growth and minimizing the influence it has on the host tree at much higher rates than *P. glauca*. If the bands are not callose deposits, it is still likely that they are the result of the host trees' wounding response and are benefiting the host tree. This is indicated by the bands' relative absence in *P. glauca* compared to *P. rubens* and given that *P. glauca* cannot survive infection while *P. rubens* can.

The histological stains used in this study, Safranin O and Aniline Blue, have been utilized to define lignin and callose in plant tissue for decades (Cochrane and Ford, 1978; Karuppaiyan et al., 2006; Kutscha and Gray, 1972; Mulyaningsih et al., 2022; Nikolov et al., 2014; Thomas et al., 1894). The different colors mapped onto components of *Picea* shoot's anatomical structure known to be high in lignin or callose (Figure 7, 8) (Karuppaiyan et al., 2006; Kutscha and Gray, 1972; Mulyaningsih et al., 2022). The phloem of plants, such as the *Picea* species sampled in the present study, are known to have greater amounts of callose than the xylem, while also

containing un-lignified cells (Calvin et al., 1984; Evert and Derr, 1964; Li et al., 2023; Montwé et al., 2019). The phloem is typically high in callose due to the controlling function of callose in the sieve tubes, not necessarily as a wounding response (Chen and Kim, 2009; Montwé et al., 2019). Both factors, high callose and low lignin, lead to the phloem staining a blue/purple color in samples under full light (Montwé et al., 2019). On the other hand, the xylem consists of specialized, lignified, cells, staining a bright red color under full light because of the application of Safranin O (Baldacci-Cresp et al., 2020; Brown, 1961; Mulyaningsih et al., 2022). By first identifying the phloem and xylem and their staining patterns, allowed the orientation of *A. pusillum* infection observations within the cross sections, enabling a more informed analysis of the host trees' responses.

Results from this study show that *P. rubens* experience the same signs of *A. pusillum* infection intensity as *P. glauca* in terms of the number of infection occurrences and the area of the infections' contained interior. The difference in outcome of infection, in terms of mortality, may be a result of the host trees response to the parasite. Data reveal that *P. rubens* trees that are infected with eastern dwarf mistletoe, respond by actively 'banding' sites of infection, significantly more frequently than *P. glauca* trees of the same condition. The exterior bands of *P. rubens* infections were significantly larger than the few exterior bands around *P. glauca* infections. The ability that *P. rubens* seems to possess to encompass the sources of infection as a wounding response is clearly lacking in *P. glauca*, possibly having a large impact on its survivability of *A. pusillum* infection (Poovaiah, 1974)

It is well documented that there are different manifestations of *Arceuthobium pusillum* infections in *P. glauca* and *P. rubens* (F. G. Hawksworth and A. L. Shigo, 1980; Hawksworth and Wiens, 1996; Logan et al., 2013; Reblin et al., 2006). In the field, these differences are largely visualized as high mortality in *P. glauca,* and differing 'witches broom' characteristics (F. G. Hawksworth and A. L. Shigo, 1980; Tinnin et al., 1982). It is known that *Picea rubens* is able to withstand infection while *Picea glauca* eventually succumbs to the *A. pusillum* infection (Eaton, 1931; F. G. Hawksworth and A. L. Shigo, 1980; Kuijt, 1955). Despite this understanding, the specific physiological mechanisms by which the infections intensities differ to such a dramatic degree across species is unknown. In an effort to bridge this gap of knowledge, this study presents an introduction into the differences between the responses of *P. rubens* and *P. glauca* to *A. pusillum* infection at the shoot anatomical level.

This study provides a framework for future analysis. To further investigate and deepen an understanding of the host-species specific differences in *Arceuthobium pusillum* infections, there are several avenues of research worth pursuing. First, it would be beneficial to histologically stain and examine the banded exteriors of infections. Examining a smaller, and thinner, tissue sample may reveal cellular qualities of the exterior bands that were absent in this study's staining of the whole branch cross section. Second, it would be interesting to experiment with other histological stains. For instance, using other stains to differentiate gymnosperms and angiosperms, such as phloroglucinol which stains for lignin, would serve to corroborate this study's results (Pradhan Mitra and Loqué, 2014). Implementing stains with different uses than the ones in this study also has the potential to further this line of inquiry by possibly identifying more characteristics of the infections in red spruce trees as they compare to those in white spruce trees. Third, and finally, it would worthwhile to quantify other conventional qualities of conifers' wounding responses. For example, conifers, and most plants, often respond to wounding with certain terpenes, which can operate as warning signals, anti-inflammatory treatments, or herbivory repellents, to name a few functions (Łukowski et al., 2022). Analyzing the concentrations of terpenes or terpene rich molecules, such as oleoresin, in red spruce trees and white spruce trees infected with eastern dwarf mistletoe, may provide information about how red spruce trees can shed infected branches and withstand infection (Celedon and Bohlmann, 2019).

Acknowledgements

I would like to thank Professor Barry Logan for his thoughtful mentorship over the course of this yearlong study. I would also like to acknowledge Professor Brett Huggett of Bates College for extending his wisdom on plant anatomy. Additionally, I would like to thank my readers, Professor Jones and Professor Douhovnikoff of Bowdoin College for their input on this project. I would also like to extend my acknowledgements and gratitude to the people of Monhegan Land and the Monhegan Island Associates for welcoming me and allowing me to sample from, the magnificent Monhegan island. This study would not have been possible without the help of these individuals listed and many others, thank you all.

Works Cited

Baker, F., O'Brien, J. G., Mathiasen, Robert, and Ostry, M.Ee (2006). Eastern Spruce Dwarf Mistletoe. *U.S. Department of Agriculture, Forest Service*.

Baldacci-Cresp, F., Spriet, C., Twyffels, L., Blervacq, A.-S., Neutelings, G., Baucher, M. and Hawkins, S. (2020). A rapid and quantitative safranin-based fluorescent microscopy method to evaluate cell wall lignification. *The Plant Journal* **102**, 1074–1089.

Barton M. Blum (1990). *Picea rubens* Sarg. In *Silvics of North America*.

Brown, S. A. (1961). Chemistry of Lignification. *Science* **134**, 305–313.

Calvin, C. L., Hawksworth, F. G. and Knutson, D. M. (1984). Phloem in *Arceuthobium globosum* (*Viscaceae*). *Botanical Gazette* **145**, 461–464.

Celedon, J. M. and Bohlmann, J. (2019). Oleoresin defenses in conifers: chemical diversity, terpene synthases and limitations of oleoresin defense under climate change. *New Phytologist* **224**, 1444–1463.

Chen, X.-Y. and Kim, J.-Y. (2009). Callose synthesis in higher plants. *Plant Signal Behavior* **4**, 489–492.

Cochrane, L. A. and Ford, E. D. (1978). Growth of a Sitka Spruce Plantation: Analysis and Stochastic Description of the Development of the Branching Structure. *Journal of Applied Ecology* **15**, 227–244.

Cogbill, A. B., Alan White, &. Charles (2013). Reconstructing the Past: Maine Forests Then and Now. In *The Changing Nature of the Maine Woods*.

Conti, G. G., Marte, M. and Leone, G. (1983). Effect of Light and Dark on Callose Deposition During the Hypersensitive Reaction in Datura Stramonium L. Infected with Tobacco Mosaic Virus. *Rivista di Patologia Vegetale* **19**, 85–97.

Currier, H. B. (1957). Callose Substance in Plant Cells. *American Journal of Botany* **44**, 478–488.

Davis, R. B. (1966). Spruce-Fir Forests of the Coast of Maine. *Ecological Monographs* **36**, 80–94.

de Lafontaine, G., Turgeon, J. and Payette, S. (2010). Phylogeography of white spruce *(Picea glauca)* in eastern North America reveals contrasting ecological trajectories. *Journal of Biogeography* **37**, 741–751.

Dodds, J. S. (2022). *Arceuthobium pusillum Rare Plant Profile*. Trenton, NJ: New Jersey Department of Environmental Protection, State Parks, Forests & Historic Sites, State Forest Fire Service & Forestry, Office of Natural Lands Management, New Jersey Natural Heritage Program.

Eaton, R. J. (1931). Peculiar Aspects of the New England Distribution of *Arceuthobium Pusillum*. *Rhodora* **33**, 92–101.

Evert, R. F. and Derr, W. F. (1964). Callose Substance in Sieve Elements. *American Journal of Botany* **51**, 552–559.

F. G. Hawksworth and A. L. Shigo (1980). Dwarf mistletoe on red spruce in the White Mountains of New Hampshire. *Plant Disease* **64**, 880–882.

Felton, A., Nilsson, U., Sonesson, J., Felton, A. M., Roberge, J.-M., Ranius, T., Ahlström, M., Bergh, J., Björkman, C., Boberg, J., et al. (2016). Replacing monocultures with mixed-species stands: Ecosystem service implications of two production forest alternatives in Sweden. *Ambio* **45**, 124–139.

Foster, D. R., Hall, B., Barry, S., Clayden, S. and Parshall, T. (2002). Cultural, environmental and historical controls of vegetation patterns and the modern conservation setting on the island of Martha's Vineyard, USA. *Journal of Biogeography* **29**, 1381–1400.

Gray, E. R., Russell, M. B., Babcock, C. and Windmuller-Campione, M. A. (2022). Structural characteristics of black spruce *(Picea mariana)* infested with eastern spruce dwarf mistletoe *(Arceuthobium pusillum)*, Minnesota, USA. *Forest Ecology and Management* **523**, 120495.

Hans Nienstaedt and John C. Zasada (1990). *Picea glauca* (Moench) Voss. In *Silvics of North America*, pp. 204–226.

Hawksworth, F. G. and Wiens, D. (1996). Dwarf mistletoes: Biology, pathology, and systematics. *Agricultural Handbook 709. Washington, D.C.: U.S. Dept. of Agriculture, Forest Service. 410 p.*

Jack, J. G. (1900). *Arceuthobium Pusillum* in Massachusetts. *Rhodora* **2**, 6–8.

Karuppaiyan, R., Nandini, K., Girija, T., Anoop, E. V. and Abdul Nizar, M. (2006). Techniques in Anatomy, Cytology and Histochemistry of Plants.

Kuijt, J. (1955). Dwarf Mistletoes. *Botanical Review* **21**, 569–627.

Kutscha, N. and Gray, J. R. (1972). TB53: The Suitability of Certain Stains for Studying Lignification in Balsam Fir, *Abies balsamea* (L.) Mill. *Life Sciences and Agriculture Experiment Station Technical Bulletin* **53**,.

Li, N., Lin, Z., Yu, P., Zeng, Y., Du, S. and Huang, L.-J. (2023). The multifarious role of callose and callose synthase in plant development and environment interactions. *Frontiers in Plant Science* **14**, 1183402.

Logan, B. A., Reblin, J. S., Zonana, D. M., Dunlavey, R. F., Hricko, C. R., Hall, A. W., Schmiege, S. C., Butschek, R. A., Duran, K. L., Emery, R. J. N., et al. (2013). Impact of eastern dwarf mistletoe *(Arceuthobium pusillum)* on host white spruce *(Picea glauca)* development, growth and performance across multiple scales. *Tree Physiology* **147**, 502–513.

Lorimer, C. G. (1977). The Presettlement Forest and Natural Disturbance Cycle of Northeastern Maine. *Ecology* **58**, 139–148.

Łukowski, A., Jagiełło, R., Robakowski, P., Adamczyk, D. and Karolewski, P. (2022). Adaptation of a simple method to determine the total terpenoid content in needles of coniferous trees. *Plant Science* **314**, 111090.

Lux, A., Morita, S., Abe, J. and Ito, K. (2005). An Improved Method for Clearing and Staining Free-hand Sections and Whole-mount Samples. *Annals of Botany* **96**, 989–996.

LYE, D. (2006). Charting the Isophasic Endophyte of Dwarf Mistletoe *Arceuthobium douglasii* (*Viscaceae*) in Host Apical Buds. *Annals of Botany* **97**, 953–963.

Montwé, D., Hacke, U., Schreiber, S. G. and Stanfield, R. C. (2019). Seasonal Vascular Tissue Formation in Four Boreal Tree Species With a Focus on Callose Deposition in the Phloem. *Front. For. Glob. Change* **2**,.

Muche, M., Muasya, A. M. and Tsegay, B. A. (2022). Biology and resource acquisition of mistletoes, and the defense responses of host plants. *Ecological Processes* **11**, 24.

Mudgal, G., Kaur, J., Chand, K., Parashar, M., Dhar, S. K., Singh, G. B. and Gururani, M. A. (2022). Mitigating the Mistletoe Menace: Biotechnological and Smart Management Approaches. *Biology* **11**, 1645.

Muir, J. A. and Hennon, P. E. (2007). *A synthesis of the literature on the biology, ecology, and management of western hemlock dwarf mistletoe.* Portland, OR: U.S. Department of Agriculture, Forest Service, Pacific Northwest Research Station.

Mulyaningsih, T., Karnika, D. A. and Muspiah, A. (2022). Comparison of stem anatomy of *Bambusa vulgaris* Schrad and *Schizostachyum brachycladum* (Kurz) Kurz (Poaceae) in Lombok. *Advances in Bamboo Science* **1**, 100010.

Nikolov, L. A., Tomlinson, P. B., Manickam, S., Endress, P. K., Kramer, E. M. and Davis, C. C. (2014). Holoparasitic Rafflesiaceae possess the most reduced endophytes and yet give rise to the world's largest flowers. *Annals of Botany* **114**, 233–242.

Norton, A. H. (1907). The Dwarf Mistletoe on the Southeastern Coast of Maine. *Rhodora* **9**, 208–208.

Nowacki, G., Carr, R. and Dyck, M. V. (2010). The current status of red spruce in the eastern United States: distribution, population trends, and environemtnal drivers. *U.S. Department of Agriculture, Forest Service*.

Poovaiah, B. W. (1974). Formation of Callose and Lignin During Leaf Abscission. *American Journal of Botany* **61**, 829–834.

Pradhan Mitra, P. and Loqué, D. (2014). Histochemical Staining of *Arabidopsis thaliana* Secondary Cell Wall Elements. *J Vis Exp* 51381.

Reblin, J. S., Logan, B. A. and Tissue, D. T. (2006). Impact of eastern dwarf mistletoe *(Arceuthobium pusillum)* infection on the needles of red spruce *(Picea rubens)* and white spruce *(Picea glauca)*: oxygen exchange, morphology and composition. *Tree Physiology* **26**, 1325–1332.

Rosier, James and Burrage, Henry, S. (1887). *Rosier's Relation of Waymouth's voyage to the coast of Maine, 1605 : with an introduction and notes*. Portland, ME: Gorges Society.

Spaulding, P. (1906). Studies on The Lignin and Cellulose of Wood. *Missouri Botanical Garden Annual Report* **1906**, 41–58.

Srebotnik, E. and Messner, K. (1994). A Simple Method That Uses Differential Staining and Light Microscopy To Assess the Selectivity of Wood Delignification by White Rot Fungi. *Applied and Environmental Microbiology* **60**, 1383–1386.

Stanton, S. (2006). The differential effects of dwarf mistletoe infection and broom abundance on the radial growth of managed ponderosa pine. *Forest Ecology and Management* **223**, 318–326.

Thoday, D. and Johnson, E. T. (1930). On Arceuthobium pusillum, Peck: I. The Endophytic System. *Annals of Botany* **44**, 393–413.

Thomas, M. B., Thomas, M. B. and Dudley, W. R. (1894). *A laboratory manual of plant histology*. Crawfordsville, Ind: [The Journal Co., Printers].

Tinnin, R. O., Hawksworth, F. G. and Knutson, D. M. (1982). Witches' Broom Formation in Conifers Infected by *Arceuthobium spp*.: An Example of Parasitic Impact upon Community Dynamics. *The American Midland Naturalist* **107**, 351–359.

Tolonen, M. (1983). Pollen evidence of vegetational change following early European settlement of Monhegan Island, Maine, northeastern U.S.A. *Boreas* **12**, 201–215.

von Schrenk, H. (1900). Notes on *Arceuthobium Pusillum*. *Rhodora* **2**, 2–5.

Wang, Y., Li, X., Fan, B., Zhu, C. and Chen, Z. (2021). Regulation and Function of Defense-Related Callose Deposition in Plants. *Int J Mol Sci* **22**, 2393.

Zhang, L., Larsson, A., Moldin, A. and Edlund, U. (2022). Comparison of lignin distribution, structure, and morphology in wheat straw and wood. *Industrial Crops and Products* **187**, 115432.